Proceedings of the Canadian Society for Mechanical Engineering International Congress
Computational Fluid Dynamics Canada International Congress
CSME - CFD-SC2023
May 28-31, 2023, Sherbrooke, QC, Canada

A Method of Evaluating ADAS Camera Performance in Rain - Case Studies with Hydrophilic and Hydrophobic Lenses

Wing Yi Pao[1*], Long Li[2], Martin Agelin-Chaab[1]
[1]Department of Mechanical and Manufacturing Engineering, Ontario Tech University, Oshawa, Canada
[2]Department of Automotive and Mechatronics Engineering, Ontario Tech University, Oshawa, Canada
*wingyi.pao@ontariotechu.net

Abstract—Advanced driver assistance systems (ADAS) are increasingly being equipped in modern vehicles to provide safety warnings and autonomous functions. Cameras are a key component in ADAS which collects critical environmental information as inputs. Similar to human vision, cameras suffer performance degradation in adverse weather conditions. The impacts of precipitation, such as raindrops on camera lenses, cause blurring and obstruction of camera vision, which subsequently affects ADAS performance. The relationships between camera image quality, object detection accuracy, and surface wettability of camera lenses are investigated for different driving-in rain conditions. The goal is to link camera performance with ADAS performance from a practical perspective. Moreover, the use of hydrophilic and hydrophobic camera lenses is explored to provide insights into material selection when designing camera lenses for ADAS. The rain characteristics perceived by a moving vehicle at different driving speeds are simulated using a patent pending rain simulation system implemented into a wind tunnel. It is found that droplet characteristics, such as size, shape, and motion, can impact the camera image quality and, subsequently, object detection accuracy. The results suggest that the use of hydrophobic camera lenses promotes better performance over hydrophilic lenses in most cases, while object detection capability is restored more effectively on the hydrophilic lens when a water film layer is formed.

Keywords-camera; sensor performance; perceived rain simulation; autonomous vehicle; object detection; image quality evaluation; soiling quantification; hydrophilic; hydrophobic

I. INTRODUCTION

Advanced driver assistance systems (ADAS) play a critical role in reducing the risk of road accidents by alerting drivers or performing autonomous tasks [1]. Cameras are one of the most common ADAS sensors, as all modern vehicles have cameras to perform various driver assistance tasks. In fact, with current technologies, it can be said that the camera is considered to be the most important sensor on a vehicle [2]. For example, Tesla, a leading manufacturer of electric vehicles that are well-known for their autopilot functions, has explored the use of only cameras, a total of eight cameras in the recent models [3], shown in Fig. 1.

A stereo-vision system can be achieved by using two or more cameras, facilitating the possibility of generating a 3-dimensional (3D) image with depth perception. Whereas when only a single camera is used, the mono-vision system results in 2-dimensional (2D) images. Today, cameras are compact, high resolution, and relatively inexpensive compared to other ADAS optical sensors (e.g., LiDARs). Many state-of-the-art ADAS features rely on camera image input, including lane departure warning, parking assist, and traffic sign recognition [2].

There has been a growing interest in autonomous vehicle (AV) developments, evidenced by various field testing announcements made by AV manufacturers. However, to this date, the performance of ADAS sensors when driving in adverse weather conditions is still not very well understood and quantified. This literature gap hinders the development of reliable and safe autonomous features for road vehicles.

In addition, it has been demonstrated that material selection is rather important in optical sensor performance. It is common for vehicle users to apply coatings on glazing surfaces, such as windshields, side windows, and mirrors, to improve visibility. Considerations of surface functionalities have a long history. A major motivation for tuning surface properties is to provide protection and passively mitigate surface contaminants (i.e., soiling). It was discussed that coatings would be a big part of future AVs, particularly for ADAS sensor applications [4].

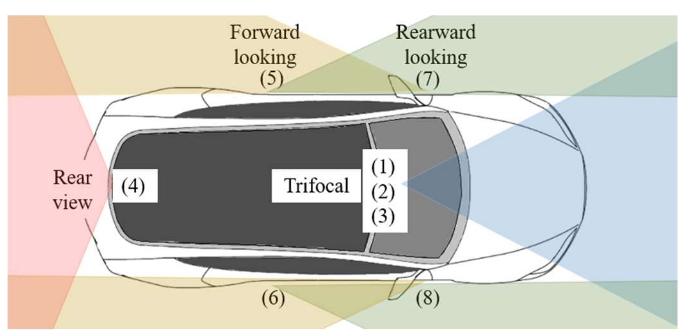

Figure 1. Locations of cameras on a Tesla vehicle.

Previously, our research group has investigated the degradation of camera focus quality when subjected to controlled wind-driven rain, which replicates the perceived rainfall conditions of a moving vehicle [5]. This paper is a continuation of the work in [5], with the intention to not only evaluate the raw camera image quality but also object detection accuracy as a step to quantify ADAS, as well as case studies with different lens materials.

The objectives of this paper are to first simulate realistic driving-in rain conditions in a controlled environment, then to evaluate camera and ADAS performances on relative clarity and object detection accuracy using existing metrics and algorithms, and lastly to investigate the effects of surface wettability of the camera lens on camera performances. The proposed studies will contribute to understanding the necessary correlations between driving-in rain conditions and the effects of lens material selection on ADAS camera performance. It is hopeful that this will aid AV developments.

II. Literature Review

A. Camera Vision in Rain

Cameras work in the visible light region, which resembles human eye perceptions. Cameras are passive sensors as they receive signals without emitting any. They have light sensors that convert the reflected light from an image onto a planar view through focusing from the lens. Camera vision in rain is highly dependent on the camera specifications, such as exposure time, depth of field, and algorithms [6]. Parameters can be selected for various purposes, such as to reduce or enhance rain effects.

Camera vision is affected by both falling droplets (in-mid-air) and adherent droplets (on the camera lens) [7]. Droplets in the atmosphere cause contrast attenuation, whereas fast moving in-air droplets cause sharp intensity changes. On the other hand, camera performance degrades when raindrops impact the lens frequently. Droplets that adhere to the lens cause distortions and blurriness; the light reflections can also cause the deterioration of operational algorithms.

B. Camera Raw Image Quality

In ADAS, an optical camera provides the ability to perceive environmental information, therefore, it is a major contributor to higher autonomy [2]. Through image processing techniques and convolutional neural network (CNN) based machine learning algorithms, object detection capability can be achieved [8]. Degradation in camera perception quality due to adverse weather conditions negatively affects the ability to detect surrounding objects [9]. In the case of driving in rain, water droplet induced degradation in the forms of blurring, glaring, and distortion to the ground truth image severely lowers the quality of detection. Therefore, maintaining a high level of camera image quality is a top priority in ensuring reliable ADAS functionalities.

It can be said that delivering high clarity raw image input is the first step in object detection quality. To quantify the quality of raw camera image, two types of evaluation metrics are often used – full reference and no reference metrics [10]. Full reference metrics such as Peak Signal-to-Noise Ratio (PSNR) and Structural Similarity Index Measure (SSIM) require a reference image as a comparison standard. No reference metrics, while only providing estimation, require no reference frame. Common no reference assessment metrics evaluate the degree of blurring or blocking and spatial and temporal information [11]. Although no agreed-upon standards exist in real world automotive applications, no reference assessment metrics are more logical to deploy due to a lack of controlled reference frames when driving outdoors.

C. Soiling Detection

In order to enhance camera image quality, some have proposed methods to support partial signal degradation using soiling detection methods; common strategies include a binary algorithm that uses annotations to determine the severity of soiling [12] or image processing approaches such as background subtraction and watershed techniques [13]. In simpler terms, the presence of degraded spots on the camera image due to adherent droplets on the camera lens is identified and can undergo corrections.

However, these proposed methods are not able to provide extremely precise information for complete restoration, where the image processing techniques could only yield around 70 % accuracy when compared to the ground truth [13]. The background subtraction method also yielded slightly higher false positive counts per image, which may lead to a counter-effect when attempting to enhance the image quality.

D. Object Detection Quality

It was debated that a lot of existing work on droplet detection is fundamentally interesting, but they are not practical from the ADAS sensor application perspective [13]. Ultimately, images obtained by the camera cannot provide any useful information if the ADAS does not recognize the information within the images. Here, object detection comes into play as the major input for various ADAS functions. The quality of object detection is necessary to be assessed to determine the feasibility of real-world implementation.

Object detection algorithms often employ CNN models. One of the most popular open-source object detection models is You Only Look Once (YOLO) [14]. The standard evaluation metric for object detection algorithms is Intersection-over-Union (IoU), defined as

$$IoU = \frac{|A \cap B|}{|A \cup B|} \tag{1}$$

IoU compares the bounding boxes of the ground truth object to the prediction bounding boxes, depicted as the overlapping area over the union area [2]. In addition to IoU, the metrics of precision and recall offer further performance quantification [15]. Precision and recalls are defined as:

$$Precision = \frac{True\ positive}{True\ positive + False\ positive} \tag{2}$$

$$Recall = \frac{True\ positive}{True\ positive + False\ negative} \tag{3}$$

Through the effort of numerous individuals across the globe over time, multiple variations of YOLO exist in the open literature, each with its pros and cons [16]. Studies to compare versions of YOLO have been performed by several research teams [17, 18].

E. Effects of Material Wettability

Droplets can be considered as liquid lenses that compound onto the camera lens at individual spots, which attenuate light paths due to their curvatures [19]. As a result, they affect camera performance. Droplet contact time is also a crucial parameter that determines the severity and duration of performance degradation. Bouncing is often seen on hydrophobic surfaces with contact time as low as 10 milliseconds but is rarely observed on hydrophilic surfaces, as droplets would spread and dissipate kinetic energy [20].

Criteria for anti-soiling surfaces were established in the past; gradually, more attention was turning towards reducing the Weber number, and increasing hydrophobicity as these surfaces showed better performance in self-cleaning ability, owing to the shape and resultant motion of the droplets [21]. However, without actual quantification of camera performance and the capability of ADAS to interpret the input information, huge assumptions remain for optical sensor performance in soiling conditions, only relying on the observations from human eye perception.

III. EXPERIMENTAL

In this study, ADAS camera performance when driving in rain is investigated. Perceived rain conditions for a moving vehicle are simulated in a wind tunnel. The rain characteristics are first measured, and the camera is exposed to the same calibrated conditions afterwards. Two camera lenses having different wettabilities, hydrophilic and hydrophobic, are investigated. Video footage is recorded during each test trial for two minutes, and then camera image quality and object detection accuracy are quantified on these files. The details of the methodology are outlined in the following sections.

A. Wind Tunnel Setup

Controlled testing is performed using an open circuit model wind tunnel, having a test section size of 40 cm (H) x 50 cm (W) x 110 cm (L). A rectangular waterproof container is used to protect the camera assembly. The side walls of the test section are removed to reduce blockage effects, and a flow-collector flap is placed at the top of the test section to prevent updraft. Improvement of the setup is made compared to the previous work by the authors [5]. The container is positioned at the center height of the test section on top of a hollow riser block, shown in Fig. 2, to eliminate the undesired boundary layer effect near the bottom board, as aerodynamics plays a significant role in the droplet dynamics.

B. Driving-in Rain Conditions

Three driving speeds (50, 75, and 100 km/h) and three rain intensities (light, moderate, and heavy rain) are studied, resulting in a total of nine test conditions. These conditions represent the range of typical driving-in rain scenarios on city, sub-urban, and highway roads. Controlled rain conditions are simulated using a patent pending (Application Number US 17/994,886) rain system with vertically dispensed raindrops above the test section; the droplets are then deflected by the horizontal wind upon entering the wind-stream.

The author' previous work [5] already demonstrated the perceived concept that driving faster generates higher raindrop

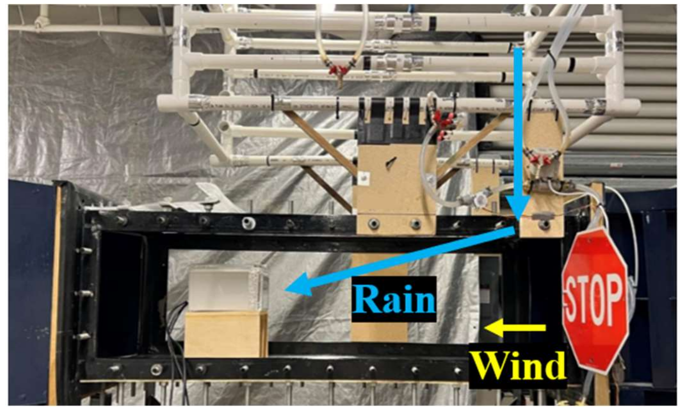

Figure 2. Experimental setup at the model wind tunnel at Ontario Tech University, Canada.

counts and intensity on the front facing camera; the same concept is applied in this study. The rain characteristics are measured with the Thies Clima Laser Precipitation Monitor (LPM), which is an optical disdrometer. The volume mean droplet diameter is measured to be between 0.66 to 1.58 mm for all the simulated conditions.

Despite optical disdrometers being one of the most advanced equipment for weather measurements, there are still a lot of uncertainties in the recorded data [22]. In the authors' previous study [5], the per-particle-event mode was used. In the present study, a per-minute-distribution mode is used to eliminate some of the data loss arising from communication in cases with higher intensity and droplet counts, which finds a better fit with the quantified camera performance.

As such, using the same previously calibrated rain system parameters, some of the intensities measured in this paper (Table 1) are different from the ones reported previously [5], and might deviate from the actual target intensities. Therefore, the dynamic to static intensity ratio is neglected, and each driving speed is treated as a separate dataset. The primary scope of the paper is to investigate the materials effect on camera performance using hydrophilic and hydrophobic lenses; the effect of driving speed is not an objective of this paper.

C. Camera and Lens Materials

The camera model used in this study is the GoPro Hero7. The camera is set with 1920 × 1440 pixels at 60 fps and linear view. The camera is placed inside the waterproof container and is fixed in angle and position. A 4.5 mm thick, flat and optically transparent cover is placed 5.0 mm in front of the camera, which acts as the outer protection lens of the device assembly.

Two different materials are investigated, including a bare acrylic (hydrophilic) and a coated acrylic with RainX-Plastic (hydrophobic). The wettabilities of the two materials are measured using the Sessile drop method [23]. The static water contact angles are ~50° and ~90° for the hydrophilic and hydrophobic variants, respectively, as shown in Fig. 3.

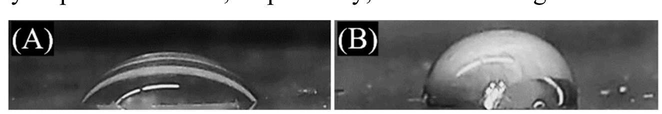

Figure 3. Droplet on the (A) hydrophilic lens and (B) hydrophobic lens.

TABLE I. PERCEIVED RAIN INTENSITIES SIMULATED FOR DIFFERENT DRIVING-IN-RAIN CONDITIONS

Rain Category	Measured Rain Intensities (mm/h)		
	50 km/h	*75 km/h*	*100 km/h*
Light	5.0	5.1	12.3
Moderate	21.0	25.2	96.3
Heavy	71.3	104.5	270.8

D. *Blurring Index Evaluation*

While full reference image quality assessment metrics are possible in this testing environment, a no reference quality assessment metric is used in this study as it better applies to real-world ADAS implementation. The MSU Blurring Index Metric, reported previously [24], estimates the power of blurring within a dataset by estimating the color variance in neighboring pixels. The Delta variation is used in this study, which computes a neighboring radius of 1-pixel. It is noted that the index score of a no reference metric is by no means absolute. The index score is used as a comparative measure to evaluate relative image quality within the dataset. The reason for selecting the MSU Blurring Index Metric is largely due to the fact that it is not restricted to measuring compression artifacts only, but also natural out-of-focus areas. Although this would lead to a limitation that only index values generated within a similarly structured dataset can be directly compared, however, the camera location and surrounding environmental information are both constant in this study. Therefore, the said limitation does not apply.

E. *Object Detection Evaluation*

To ensure a consistent object detection evaluation, a generic stop-sign is used as the realistic target for AV applications. The stop sign is placed on the outside of the wind tunnel test section, and is securely mounted without vibration. The open-source object detection model YOLOv3 is employed together with the generic and pretrained COCO dataset [25]. Using the unmodified dataset provides a bias-free evaluation platform for this study, as any training will induce an intentional improvement of the assessment. Since reducing total object classification will result in a modification of the detection quality, all other object classes in the dataset are hidden from view but not removed. Quantitative analysis is performed on the stop sign only.

The overall YOLO detection system consists of three stages: image compression or resizing, CNN computation, and outputting resultant detection as bounding boxes, classes, and confidence levels [26]. Each type of object is considered a class. The class confidence score relates to the probability of the specific class appearing in a bounding box and how well they fit the object.

In this study, quantitative analysis is performed based on several metrics: prediction confidence, IoU, precision, and recall. The prediction confidence index is generated by the detection algorithm and is then compared to the IoU of the ground truth. Fig. 4 shows a graphical representation of IoU. The overall prediction quality can be mathematically represented as:

$$Predictions\ Quality = Confidence * IoU_{Ground\ Truth} \quad (4)$$

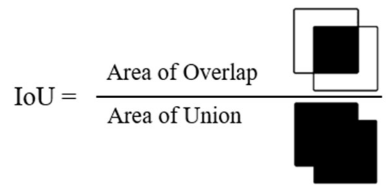

Figure 4. Definition of Intersection over Union (IoU).

Additionally, precision and recall are based on true or false and positive or negative detections. The four possible scenarios can be arranged in a confusion matrix, shown in Table 2; The four possible scenarios can be graphically represented in Fig. 5.

IV. RESULTS AND DISCUSSIONS

A. *Soiling Behaviors*

Example images from the recorded camera footage when using hydrophilic and hydrophobic lenses under 50 km/h light rain, 75 km/h moderate rain, and 100 km/h heavy rain conditions are presented in Fig. 6. Observations on the post-impact droplet dynamics are summarized.

On the hydrophilic lens, the adherent droplets are larger in size, and some are irregular in shape. Droplet movements tend to be slower and spread due to the high adsorption energy of the surface. When rain intensity is heavy enough, a layer of water film is formed. On the other hand, the adherent droplets on the hydrophobic lens are smaller in size and rounder in shape with little to no deformation. In this case, molecular interactions are higher due to low surface energy. This non-wetting effect, therefore, facilitates the drainage of water.

All observations align well with the general understanding of wettability effect on droplet behaviors [21]. This evidence is applied for further analysis and reasoning for the quantified camera image quality and object detection accuracy.

B. *Blurring Index*

The blurring index results of all tested conditions are shown in Fig. 7. It is observed that as the rain intensity increases, the image becomes more blurred. This trend is followed by both hydrophobic and hydrophilic lenses. The hydrophobic lens

TABLE II. CONFUSION MATRIX DESCRIBING THE FOUR POSSIBLE SCENARIOS IN DETECTION

	Ground truth	
Positive prediction	True positive	False negative
Negative prediction	False negative	True negative

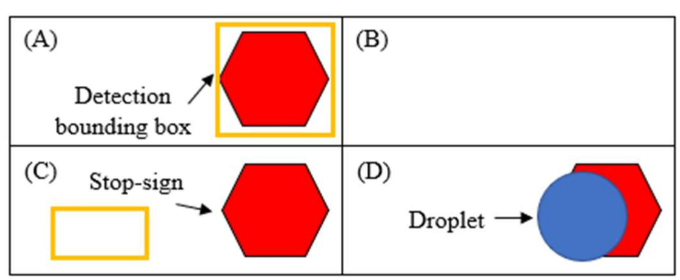

Figure 5. Definitions for (A) true positive, (B) true negative, (C) false positive, and (D) false negative.

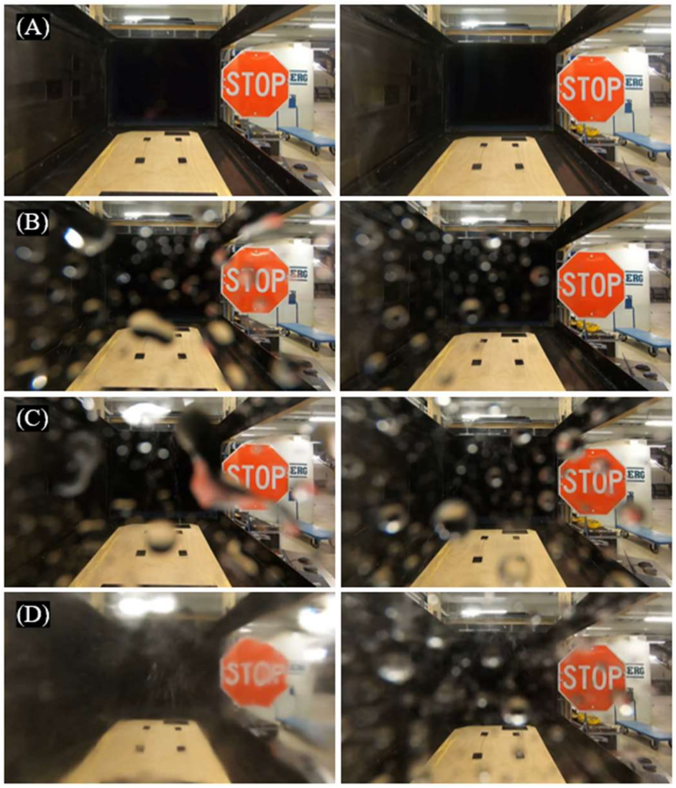

Figure 6. Example images of hydrophilic lens (left) and hydrophobic lens (right) under (A) dry, (B) 50 km/h light rain, (C) 75 km/h moderate rain, (D) 100 km/h heavy rain conditions.

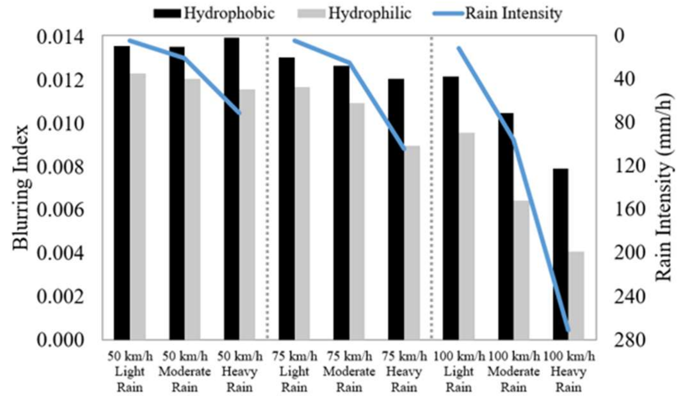

Figure 7. Blurring index scores for hydrophobic and hydrophilic lenses compared with simulated perceived rain intensities at different driving speeds.

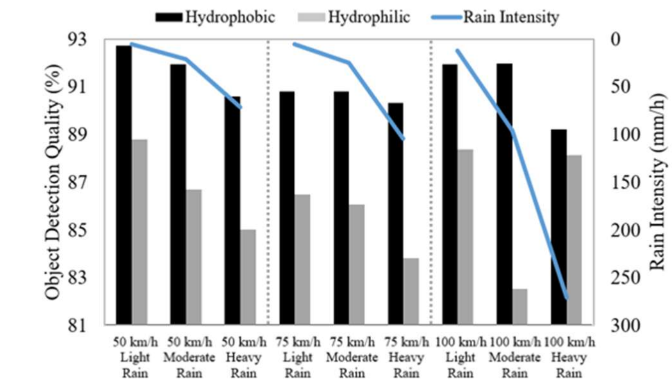

Figure 8. Prediction quality for hydrophobic and hydrophilic lenses compared with simulated perceived rain intensities at different driving speeds.

shows a steady improvement over the hydrophilic lens for all test conditions. This behavior aligns with real life observations that the application of commercially available hydrophobic coatings reduces droplet adhesion and other random interactions between nearby droplets at the glazing surfaces. Whereas hydrophilic lens induces irregularly shaped droplets, which results in distortion spots on the image. In extreme cases, water film formation is observed on the hydrophilic lens, causing significantly increased blurriness. The water film acts as a natural blurring filter and reduces contrast, or color variance, between objects, leading to a lower blurring index score. This observation is seen across all simulated driving speeds at respective perceived rain intensities. As the perceived rain condition worsens, the difference between hydrophilic and hydrophobic lenses magnifies, from 8.2% at 50 km/h light rain to 47.7% difference at 100 km/h heavy rain condition.

C. Object Detection

Object detection quality results repeated similar overall trends, demonstrated in Fig. 8. Prediction quality decreases as the perceived intensity increases. This is found true for both material lenses at various driving speeds with the exception being the case of 100 km/h heavy rain condition for the hydrophilic lens, where the object detection quality increases to a comparable degree with 100 km/h light rain. Due to the high rain intensity and high wind speed, a water film is formed and stays in a relatively stable state on the hydrophilic lens. It is suspected that this phenomenon allows the light beams to travel through the layer of water film without significant refraction.

Compared to the hydrophilic lens, the hydrophobic lens shows improvements in detection quality. However, the relationship is found to be non-linear. The increase in adherent droplet movement speed and the reduction in droplet size both contribute to reducing the overall blurriness of the image and allowing better detection of environmental information. However, a direct vision blockage by the droplets may occur in the place of blurring due to the increase in the slope of the droplet curvature. The general trend of detection quality decrease aligns with the trend of a decrease in the blurring index score. It can be said that the object detection quality depends on the camera image input clarity.

Precision represents the correctness of predictions, whereas recall represents the capability of a positive detection. Fig. 9 and Fig. 10 show the precision and recall metrics of hydrophobic and hydrophilic lenses under all tested conditions, respectively. It is found that the hydrophobic lens results in very high scores in both precision and recall, which are significantly higher than those for the hydrophilic lens. This indicates the hydrophilic lens encounters far more false positive and false negative detections, which explains the result in an overall decrease in detection quality. In the case of the hydrophobic lens, an almost perfect recall metric score is observed, a dramatic increase over the hydrophilic lens. It is suspected that the observation is due to hydrophilic cover results in larger droplets that may cause reflection, distortion, obstruction, or a combination of the three factors.

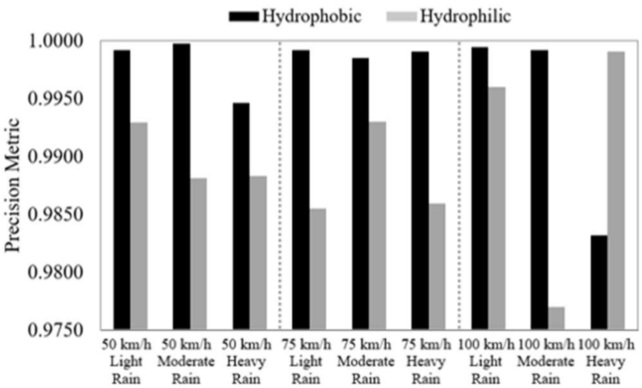

Figure 9. Precision for hydrophobic and hydrophilic lenses.

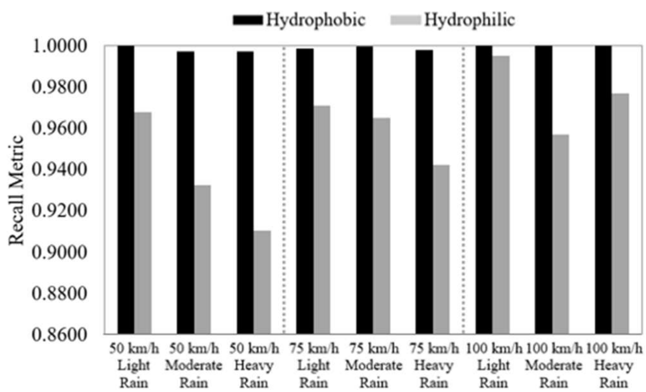

Figure 10. Recall for hydrophobic and hydrophilic lenses.

V. CONCLUSIONS

A controlled and realistic method to evaluate and quantify ADAS camera performance in various driving-in rain conditions is presented. The relationships between camera image quality, object detection accuracy, and perceived rain conditions are investigated. The proposed study serves as a step forward to correlate raw sensor signals with ADAS functionality when driving in rain. In addition, the effects of surface material properties on optical sensor performance are emphasized, which is an important parameter to be considered when conducting studies on optical sensors. This piece of information related to materials is currently lacking in the open literature. In general, camera image and object detection quality degrade as rain intensity increases. Hydrophobic lenses show more superior performance than hydrophilic lenses with higher precision and fewer false detections, except for the single case when a water film is formed and restored performance partially.

A larger database on ADAS and sensor performances is certainly desired for AV developments. Several aspects of future work are recommended, including investigating more realistic targets at different distances from the camera and with wider selections of evaluation metrics, further quantification of droplet dynamics under a broader range of conditions to aid material design and selection, as well as developing performance enhancing methods through soiling mitigation and training of object detection models in rain.

ACKNOWLEDGMENT

We acknowledge the support of the Natural Sciences and Engineering Research Council of Canada (NSERC).

REFERENCES

[1] Highway Loss Data Institute, “Predicted Availability and Fitment of Safety Features on Registered Vehicles,” Bulletin 34, no. 28, 2017, Arlington, VA

[2] P. Pathrose, ADAS and Automated Driving: A Practical Approach to Verification and Validation, SAE International, 2022.

[3] AutoPilot Review, “LiDAR vs. Cameras for Self Driving Cars - What's Best?,”2023. https://www.autopilotreview.com/lidar-vs-cameras-self-driving-cars/

[4] C. M. Seubert and Ford Research and Innovation Center, “The Future of Coatings in a World of Autonomous Vehicles,” CoatingsTech, vol. 14, no. 2, February 2017.

[5] W. Y. Pao, L. Li, M. Agelin-Chaab, “Wind-Driven Rain Effects on Automotive Camera and LiDAR Performances,” Proceedings of the Canadian Society for Mechanical Engineering (CSME) International Congress, 2022.

[6] K. Garg and S. K. Nayar, “When Does a Camera See Rain?,” 10th IEEE International Conference on Computer Vision (ICCV'05), vol. 1, December 2005.

[7] M. Roser, J. Kurz, A. Geiger, “Realistic Modeling of Water Droplets for Monocular Adherent Raindrop Recognition Using Bezier Curves,” Computer Vision Conference (ACCV), pp. 235-244, 2010.

[8] J. Ciberlin, R. Grbic, N. Teslic, M. Pilipovic, “Object Detection and Object Tracking In Front of the Vehicle Using Front View Camera,” Zooming Innovation in Consumer Technologies Conference, 2019.

[9] S. You, R. T. Tan, R. Kawakami, K. Ikeuchi, “Adherent Raindrop Detection and Removal in Video,” IEEE Conference on Computer Vision and Pattern Recognition, 2013.

[10] S. Dutta, S. D. Das, N. A. Shah, “Can No-reference Features Help in Full-reference Image Quality Estimation?,” arXiv:2203.00845, 2022.

[11] V. Kamble, K. M. Bhurchandi, “No-reference Image Quality Assessment Algorithms: A Survey,” Optik - International Journal for Light and Electron Optics, vol. 126, pp. 1090-1097, 2015.

[12] M. Uřičář, P. Křížek, G. Sistu, S. Yogamani, “SoilingNet: Soiling Detection on Automotive Surround-view Cameras,” Proceedings of IEEE Intelligent Transportation Systems Conference (ITSC), pp. 67-72, October 2019.

[13] A. Cord and N. Gimonet, “Detecting Unfocused Raindrops: In-Vehicle Multipurpose Cameras,” IEEE Robotics & Automation Magazine vol. 21, no. 1, pp. 49-56, 2014.

[14] J. Redmon, S. Divvala, R. Girshick, A. Farhadi, “You Only Look Once: Unified, Real-Time Object Detection,” arXiv, 2016.

[15] D. Powers, “Evaluation: From Precision, Recall and F-Factor to ROC, Informedness, Markedness & Correlation,” International Journal of Machine Learning Technology, vol. 2, no. 1, pp. 37-63, 2011.

[16] P. Jiang, D. Ergu, F. Liu, Y. Cai, B. Ma, “A Review of Yolo Algorithm Developments,” Procedia Computer Science, vol. 199, pp. 1066-1073, 2022.

[17] P. Adarsh, P. Rathi, M. Kumar, “YOLO v3-Tiny: Object Detection and Recognition Using One Stage Improved Model,” 6th International Conference on Advanced Computing and Communication Systems (ICACCS), pp. 687-694, 2020.

[18] S. Wang, “Research Towards Yolo-Series Algorithms: Comparison and Analysis of Object Detection Models for Real-Time UAV Applications,” Journal of Physics: Conference Series, vol. 1948, 2021

[19] W. M. Lee, A. Upadhya, P. J. Reece, T. G. Phan, "Fabricating Low Cost and High Performance Elastomer Lenses Using Hanging Droplets," Biomedical Optics Express, vol. 5, issue 5, pp. 1626-1635, 2014.

[20] X. Yu, Y. Zhang, R. Hu, X. Luo, "Water Droplet Bouncing Dynamics," Nano Energy, vol. 81, March 2021.

[21] M. Khodaei, M. 2019. “Introductory Chapter: Superhydrophobic Surfaces - Introduction and Applications,” In Superhydrophobic Surfaces: Fabrications to Practical Applications, edited by M. Khodaei, X. Chen, H. Li. London: IntechOpen, 2019.

[22] M. Angulo-Martínez, S. Beguería, B. Latorre, M. Fernández-Raga, "Comparison of Precipitation Measurements by OTT Parsivel and Thies LPM Optical Disdrometers," Hydrology and Earth System Sciences, vol. 22, issue 5, pp. 2811-2837, 2018.

[23] T. Djebbar and E. C. Donaldson, Petrophysics 4th ed. Theory and Practice of Measuring Reservoir Rock and Fluid Transport Properties. Chapter 6, Wettability, pp. 319-357, Gulf Professional Publishing, 2016.

[24] Video Processing, Compression and Quality Research Group, Computer Graphics and Multimedia Laboratory, Moscow State University, Russia, “MSU Quality Measurement Tool: Metrics Information,” Video Processing. https://videoprocessing.ai/vqmt/metrics/.

[25] T. Y. Lin, M. Maire, S. Belongie, J. Hays, et al., “Microsoft COCO: Common Objects in Context,” arXiv:1405.0312., 2015.

[26] J. Redmon, S. Divvala, R. Girshick, A. Farhadi, “You Only Look Once: Unified, Real-Time Object Detection”, arXiv:1506.02640, 2016